Cyclooxygenase-2 Overexpression in Human Basal Cell Carcinoma Cell Line Increases Antiapoptosis, Angiogenesis, and Tumorigenesis

Jeng-Wei Tjiu[1,4], Yi-Hua Liao[1,4], Sung-Jan Lin[1], Yi-Ling Huang[1], Wei-Ling Tsai[1], Chia-Yu Chu[1,2], Min-Liang Kuo[2] and Shiou-Hwa Jee[1,3]

Cyclooxygenase-2 (COX-2) is critical for tumor formation, angiogenesis, metastasis, and prognosis. In this study, the role of COX-2 in antiapoptosis, tumorigenesis, and angiogenesis of human basal cell carcinoma (BCC) cells was investigated. Transfection of COX-2 constitutive expression vector into a BCC cell line yielded several overexpressing clones. All transfectants demonstrated remarkable resistance to ultraviolet B-induced apoptosis (confirmed by flow cytometry analysis, morphological change, and DNA fragmentation). Immunoblot analysis revealed marked increases in apoptosis-regulated genes Mcl-1 and Bcl-2. A 10-fold concentrated conditioned medium from COX-2-overexpressing BCC cells exhibited higher angiogenic activity in Matrigel plug and human umbilical vein endothelial cell tube formation assay. Cells exhibited increased levels of vascular endothelial growth factor-A (VEGF-A) mRNA and protein, and secreted VEGF-A and basic fibroblast growth factor (bFGF). COX-2-specific small interfering RNA markedly reduced the secreted species. After 7 weeks of inoculation, the tumor volume of COX-2-overexpressing cells in severe combined immunodeficient mice was significantly greater than that of vector control cells. Immunohistochemical analysis of CD31-positive vessels revealed a two-fold increase in microvessel density in COX-2 tumors, compared to control vector tumors. Our data indicate that Mcl-1 and Bcl-2, as well as VEGF-A and bFGF, are downstream effectors of COX-2-induced antiapoptosis and angiogenesis, respectively.

Journal of Investigative Dermatology (2006) **126,** 1143–1151. doi:10.1038/sj.jid.5700191; published online 9 March 2006

INTRODUCTION

Cyclooxygenase (COX) is the key enzyme that mediates the production of prostaglandins from arachidonic acid. So far, two COX isoforms (cyclooxygenase-1 (COX-1) and cyclooxygenase-1 (COX-2)) have been identified. COX-1 is expressed constitutively, whereas COX-2 is induced by growth factors, tumor promoters, and cytokines (Taketo, 1998). To date, COX-2 has been determined to contribute to tumorigenesis and the malignant phenotype of tumor cells via the inhibition of apoptosis, increased angiogenesis and invasiveness, and modulation of inflammation and immunosuppression (Dempke *et al.*, 2001).

Ultraviolet B (UVB, wavelength 290–320 nm) irradiation is a major etiologic factor in the pathogenesis of non-melanotic skin cancers, including squamous cell carcinoma and basal cell carcinoma (BCC) (de Gruijl *et al.*, 2001). More than one million new non-melanotic skin cancers occur in the United States annually, with the majority of them comprising BCC (Miller and Weinstock, 1994). COX-2 and prostaglandin E2 (PGE_2) expressions in human skin are increased after UVB irradiation, especially in aged skin (Seo *et al.*, 2003). Cultured human keratinocytes display increased COX-2 protein level and PGE_2 excretion after UVB irradiation (Muller-Decker *et al.*, 1995; Buckman *et al.*, 1998). Experimentally, increases in COX-2 expression and proliferation of basal layer keratinocytes have been demonstrated in Skh-1 hairless mice after UVB irradiation (Fischer *et al.*, 1999). Reductions in UVB-induced skin papilloma or carcinoma occur upon feeding the mice with celecoxib (a selective COX-2 inhibitor) or indomethacin. Topical application of celecoxib also inhibits chronic inflammation and UVB-induced papilloma/carcinoma in Skh/hr hairless mice (Wilgus *et al.*, 2003). The ratio of squamous cell carcinoma to papillomas increases

[1]*Department of Dermatology, National Taiwan University Hospital, National Taiwan University College of Medicine, Taipei, Taiwan;* [2]*Laboratory of Molecular and Cellular Toxicology, Institute of Toxicology, National Taiwan University College of Medicine, Taipei, Taiwan and* [3]*Department of Dermatology, National Taiwan University College of Medicine, Taipei, Taiwan*

[4]*These authors contributed equally to this work*

Correspondence: Dr Shiou-Hwa Jee, Department of Dermatology, National Taiwan University Hospital and College of Medicine, National Taiwan University, 7, Chung-Shan South Road, Taipei, Taiwan.
E-mail: shiouhwa@ha.mc.ntu.edu.tw

Abbreviations: BCC, basal cell carcinoma; bFGF, basic fibroblast growth factor; CM, conditioned medium; COX-2, cyclooxygenase-2; HUVEC, human umbilical vein endothelial cell; PBS, phosphate-buffered saline; PGE2, prostaglandin E2; SCID, severe combined immunodeficiency; UVB, ultraviolet B; VEGF-A, vascular endothelial growth factor-A

Received 16 November 2005; revised 16 November 2005; accepted 11 December 2005; published online 9 March 2006

markedly in the skin of COX-2-overexpressing transgenic mice treated with the known carcinogen 7,12-dimethylbenz[a]anthracene (Muller-Decker *et al.*, 2002).

A previous immunohistochemical study described BCC to be COX-2 negative (Vogt *et al.*, 2001). Several other published reports show BCC to be COX-2 positive in a low percentage of tested biopsies (Muller-Decker *et al.*, 1999; Kagoura *et al.*, 2001; Akita *et al.*, 2004). However, a recent publication by O'Grady *et al.* (2004) demonstrated that COX-2 expression level correlated with angiogenesis in BCC specimens taken from renal transplant recipients and immunocompetent patients. Genetic and pharmacological evidence suggests that overexpression of COX-2 is critical for epithelial carcinogenesis. The purpose of the present study, therefore, was to investigate the effects of COX-2 overexpression on BCC cell apoptotic regulation, tumorigenesis, and angiogenesis. The cell regulators involved in apoptosis and angiogenesis were subsequently examined.

RESULTS

COX-2 overexpression induces resistance to apoptosis in human BCC cell line

The human COX-2 constitutive expression plasmid pCMV-COX-2 and the control vector pcDNA were transfected into human BCC cell line cells, which have a relatively low level of COX-2. After transfection, cells were cultured in a medium containing 100 μg/ml neomycin. Four stable clones (designated as B4, C5, E4, and G7) were selected, based on their increased expression of COX-2 mRNA and protein compared with the vector control cells (Figure 1a and b). Elevated levels of PGE_2 production were found in clones B4 and G7, which expressed the highest levels of COX-2 (Figure 1c).

Several apoptosis assays were performed to investigate whether COX-2 overexpression confers antiapoptotic ability to the human BCC cell line. A sensitive ELISA that measures cytoplasmic histone-associated DNA fragments further confirmed that pcDNA clone (vector control) had a higher rate of apoptosis than COX-2-overexpressing clones (B4 and G7) at 12 hours after UVB irradiation. Enrichment factors were 12.27 ± 0.32, 4.67 ± 0.43, and 4.20 ± 0.73 (expressed as mean $\pm$ SD) for pcDNA, B4, and G7, respectively ($P < 0.005$ for B4 *vs* pcDNA and $P < 0.005$ for G7 *vs* pcDNA) (Figure 2a). There was no significant variation in enrichment factors among pcDNA clone and COX-2-overexpressing clones (B4, G7) at 6 hours. Flow cytometric analysis also showed a significantly higher percentage of apoptotic cells in pcDNA than COX-2-overexpressing clones (pcDNA *vs* B4, $P < 0.001$; pcDNA *vs* G7, $P < 0.05$) (Figure 2b). Apoptotic cells were distinguished by staining with Hoechst 33258 fluorescent dye, which discerns chromatin condensation and nuclear segmentation, as an additional apoptosis assessment. As shown in Figure 2c, B4 and G7 cells had fewer apoptotic cells than the vector control cells when exposed to UVB irradiation.

The expression levels of the Bcl-2 family proteins were examined to identify possible downstream genes regulated by COX-2. Figure 3 reveals that the level of Mcl-1 protein was increased three- to four-fold in COX-2-overexpressing stable clones as compared with the vector control clone, and the level of Bcl-2 protein increased by 1.8- to 2.6-fold in

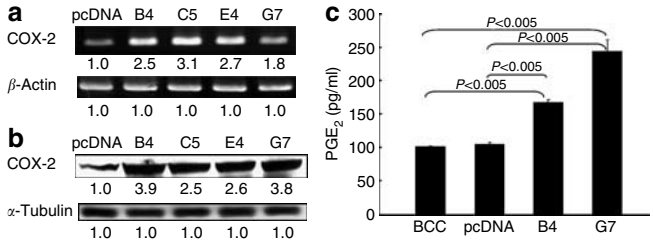

Figure 1. Determination of COX-2 mRNA, protein, and secreted PGE_2 levels in COX-2-transfected BCC cells. (**a**) The mRNA of various cell lines as indicated was extracted and semiquantified by reverse transcriptase-PCR of COX-2. (**b**) The protein extracted from cell lysates was quantified by Western blotting for COX-2. (**a**, **b**) The number below each lane indicates the relative densitometric intensity to control (defined as 1.0). This represents one of three experiments. (**c**) The secretion of PGE_2 in culture supernatant was measured by ELISA. Concentration of PGE_2 was expressed as mean $\pm$ SD in five experiments. Student's *t*-test was used for comparison. pcDNA: vector control; B4, C5, E4, and G7: clones of COX-2 transfectants.

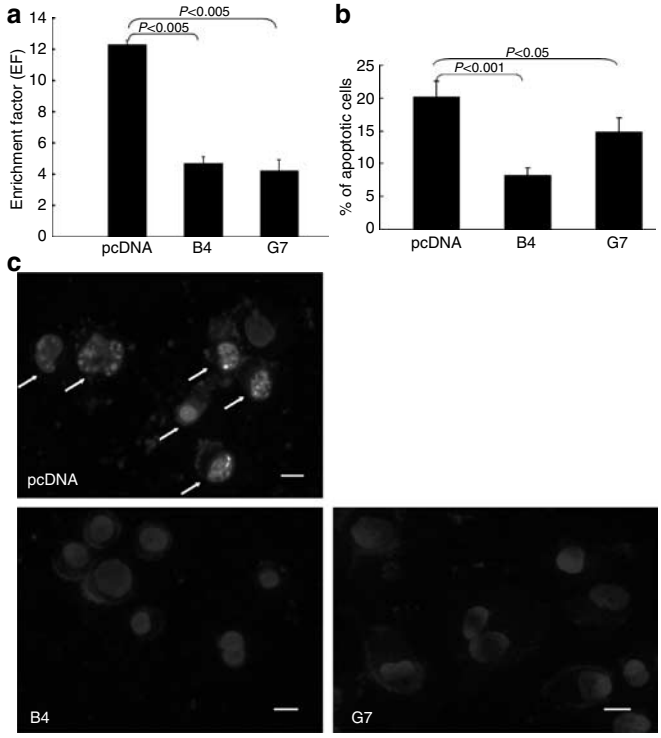

Figure 2. Expression of COX-2 protects BCC cells against apoptosis. (**a**) The cell apoptosis was measured by cell death ELISA. Enrichment factor (EF) was defined as mU of sample (12 hours after UVB irradiation)/mU of the negative control (without UVB irradiation) (mU = absorbance (10^{-3})). (**b**) Flow cytometric analysis with propidium iodide staining. (**c**) Nuclear fragmentation and chromatin condensation (arrow) determined by staining with Hoechst 33258 fluorescent dye. Each cell line was treated with 25 mJ/cm^2 UVB, and harvested at 12 hours (**a**) and at 24 hours (**b**, **c**). Data are expressed as mean $\pm$ SD in (**a**, **b**). (**c**) One of three reproducible experiments. Student's *t*-test was used for comparison ($n = 3$). pcDNA: vector control; B4 and G7: COX-2-overexpressing BCC clones. Bar = 10 μm.

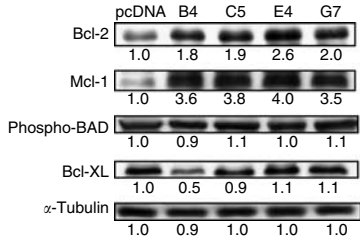

Figure 3. Immunoblot analysis of Mcl-1, Bcl-2, Bcl-XL, and phosphor-BAD proteins in different COX-2-expressing cell lines. Cell lysates were prepared and immunoblotting was performed as described in Materials and Methods. Equal aliquots of protein extracted from pcDNA, B4, C5, E4, and G7 clones were electrophoresed, and the proteins were transferred to a nitrocellulose support. The nitrocellulose was probed with specific antibodies as indicated. The number below each line indicates the relative densitometric density to control (defined as 1.0). This represents one of three reproducible experiments. pcDNA: vector control; B4, C5, E4, and G7: COX-2-overexpressing BCC clones.

COX-2-expressing clones. In contrast, the levels of the other Bcl-2 family members phospho-BAD and Bcl-XL were not significantly affected in COX-2 stable clones.

COX-2 overexpression increases angiogenesis both *in vitro* and *in vivo*

The effect of COX-2 on angiogenesis *in vitro* was initially examined by tube formation of human umbilical vein endothelial cells (HUVECs) cultured with conditioned medium (CM). Formation of the network-like tubular HUVEC structure involves the migration, invasion, and differentiation of endothelial cells. The CM obtained from the COX-2-overexpressing clones B4 and G7 showed increased tube formation per microscopic field as compared to controls (10.4 ± 1.78, $P < 0.0005$ for B4 and 10.2 ± 1.78, $P < 0.0005$ for G7 clone *vs* 0 for the vector control) (Figure 4a and b).

The effect of COX-2 on the induction of angiogenesis was assessed *in vivo* using the Matrigel plug assay. Upon visual examination, substantial vasculature was evident in plugs embedded with CM from COX-2-overexpressing BCC cells, even with hemorrhaging in the plugs, as compared to vector controls (Figure 4c). The B4 and G7 clones showed significant increases in hemoglobin relative to the control (4.55 ± 1.7 mg hemoglobin/mouse for B4, 4.32 ± 2.5 mg hemoglobin/mouse for G7 *vs* 0.22 ± 0.16 hemoglobin mg/mouse for control) (both $P < 0.05$) (Figure 4d).

The observation that COX-2 induced angiogenesis in mice prompted the study of COX-2-transfected BCC cells to determine their expression of angiogenic factors. Reverse transcriptase-PCR and immunoblotting were employed to analyze the expression of angiogenic factors including IL-8, vascular endothelial growth factor-A (VEGF-A), basic fibroblast growth factor (bFGF), and platelet-derived growth factor. As shown in Figure 5a, the expression of VEGF-A mRNA in COX-2-transfected BCC cells was higher than in vector control cells. The expression of IL-8 mRNA was also slightly increased in COX-2-overexpressing clones (varying from 1.1- to 1.6-fold). Immunoblotting analysis showed that COX-2-overexpressing BCC cells expressed more abundant

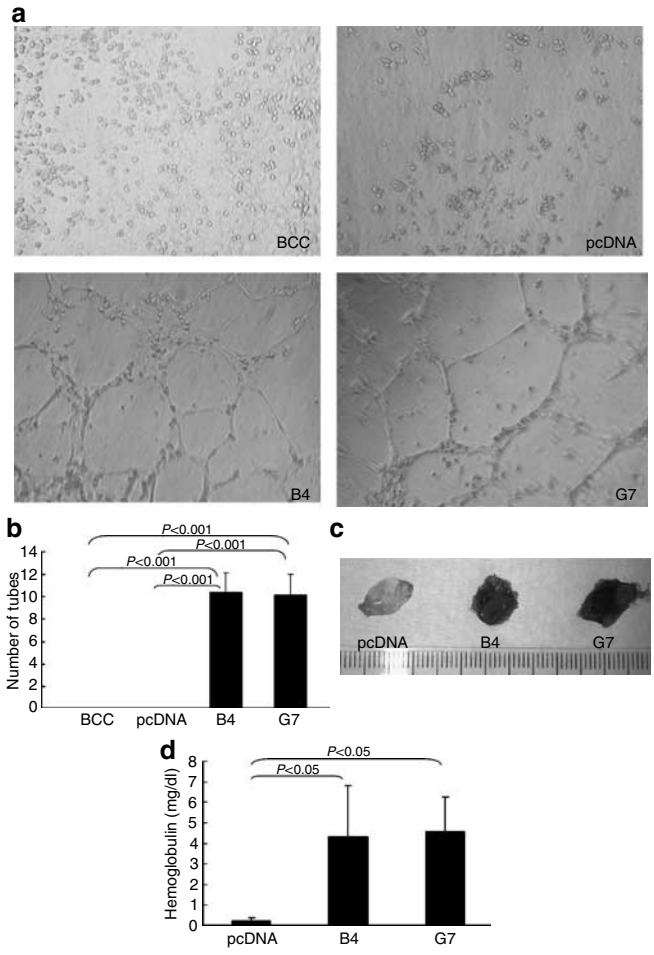

Figure 4. COX-2 overexpression increases angiogenesis both *in vivo* and *in vitro*. (**a**) Ten times concentrated culture supernatants (CM) collected from COX-2 transfectants and vector control incubated with HUVECs as depicted. (**b**) The number of tube-like structures was expressed as the mean ± SD following a random count of five 9.7 mm^2 microscopic fields. (**c**) CM from the COX-2-overexpressing clones and vector control were used for Matrigel blood plug assay in C57BL6j mice (five per group). The mice were killed 7 days after implantation. Gross appearance of the plugs was photographed. (**d**) The blood plugs were extracted and quantitation of hemoglobin was performed using the Drabkin method. The mean amount of hemoglobin was calculated. Student's *t*-test was used for comparison. Bar = 100 μm.

VEGF-A than vector controls (Figure 5b). Secreted levels of VEGF-A and bFGF were also increased significantly in B4 and G7 clones in comparison with vector control or parent BCC cells ($P < 0.0001$) (Figure 5c).

A loss-of-function assay was performed by blocking COX-2 function using COX-2-specific siRNA. Protein levels of COX-2 reduced by 51.7% and secreted PGE_2 decreased by 57.38 % in COX-2-overexpressing clones transiently transfected with COX-2-specific siRNA, which confirmed the knockdown effect of RNA interference (data not shown). The B4 and G7 clones showed statistically significant decreases in both secreted VEGF-A (54 and 56.8%, respectively) and bFGF (74 and 47.5%, respectively) after being transiently transfected with COX-2-specific siRNA (Figure 5d).

The COX-2-specific inhibitor NS-398 was also used to demonstrate specificity of the COX-2 transfection effects, and the secreted levels of PGE_2 were decreased by 90.3% in B4 clone and by 91.1% in G7 clone after 25 μM NS-398 treatment for 24 hours (data not shown). The B4 and G7 clones showed significant decreases in the secreted levels of VEGF-A (59.0 and 68.%, respectively) and bFGF (86.3 and 81.8%, respectively) after treatment with 25 μM NS-398 for 24 hours (Figure 5e).

Increased tumor growth and tumor angiogenesis in BCC cells with COX-2 overexpression in SCID mice

To compare the cell transformation ability of COX-2 transfectants and vector control cells, we employed a soft agar growth assay. A total of 1×10^3 cells from pcDNA, B4, and G7 clones were seeded into soft agar plate and colony numbers were counted 28 days after seeding. The results showed 9.2 ± 2.0, 24.7 ± 3.7, and 25.8 ± 5.4 colonies in a high-power field ($\times 200$) for pcDNA, B4, and G7 respectively (B4 *vs* pcDNA, $P<0.001$; G7 *vs* pcDNA, $P<0.001$) (Figure 6a). Microscopic examination also revealed that both B4 and G7 clones showed colonies much larger than those of the pcNDA clone (Figure 6b).

Tumorigenicity of COX-2-overexpressing clones and vector control cells in severe combined immunodeficient (SCID) mice model was next explored. Cells from pcDNA, B4, and G7 (5×10^6 each) were subcutaneously injected into 5-week-old SCID mice. The mean tumor size in G7-transplanted SCID mice was approximately 6,833 mm^3 on day 47. The B4 xenograft reached a mean of 4,377 mm^3 on day 47. In contrast, the mean tumor volume in SCID mice injected with pcDNA cells reached only a mean of 1,821 mm^3 by the same day ($P=0.0097$) (Figure 7a and b). The xenograft volume reached a statistically significant difference 22 days after implantation ($P=0.0231$). Immunohistochemical analysis of xenograft resection specimens confirmed that COX-2 staining was higher in COX-2-overexpressing clones (data not shown).

The number of blood vessels in COX-2-overexpressing xenograft tumors was quantified. A correlation was evident

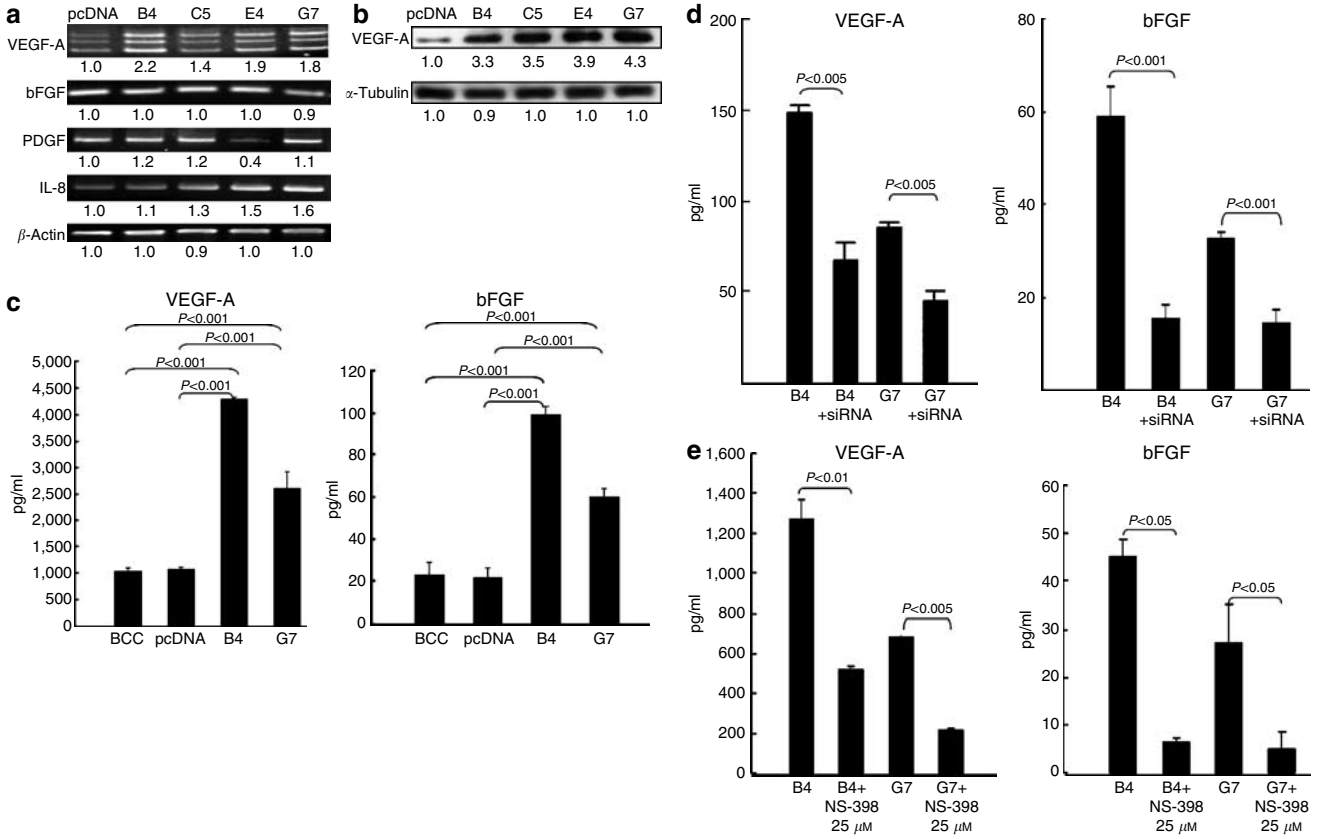

Figure 5. Expression of angiogenic factors in COX-2-transfected BCC cells. (**a**) Reverse transcriptase-PCR analysis of the level of VEGF-A, bFGF, platelet-derived growth factor, and IL-8 mRNA in COX-2 transfectants (B4, C5, E4, and G7) and vector control (pcDNA) cells. (**b**) Western blot analysis of VEGF-A protein in COX-2-overexpressing and vector control BCC cells. (**c–e**) Changes of secreted VEGF-A and bFGF were measured by ELISA. Concentrations of VEGF-A and bFGF were expressed as the mean $\pm$ SD of three independent experiments. Student's *t*-test was used for statistical analysis (**c–e**). Different culture conditions were used. (**c**) A total of 2×10^5 cells of BCC, pcDNA, B4, and G7 clones were seeded in 1.6 cm diameter culture plates, and the supernatants were collected at 48 hours. (**d**) A total of 3×10^5 cells of B4 and G7 clones were seeded in 10 cm diameter culture dishes and transiently transfected with COX-2-specific siRNA. Culture supernatants were collected at 48 hours for ELISA after siRNA transfection. (**e**) A total of 2×10^5 cells of B4 and G7 were seeded in 1.6 cm diameter culture dishes, and cultured with 25 μM of NS-398 (COX-2-specific inhibitor). Supernatants were collected for ELISA at 24 hours after supplement of NS-398.

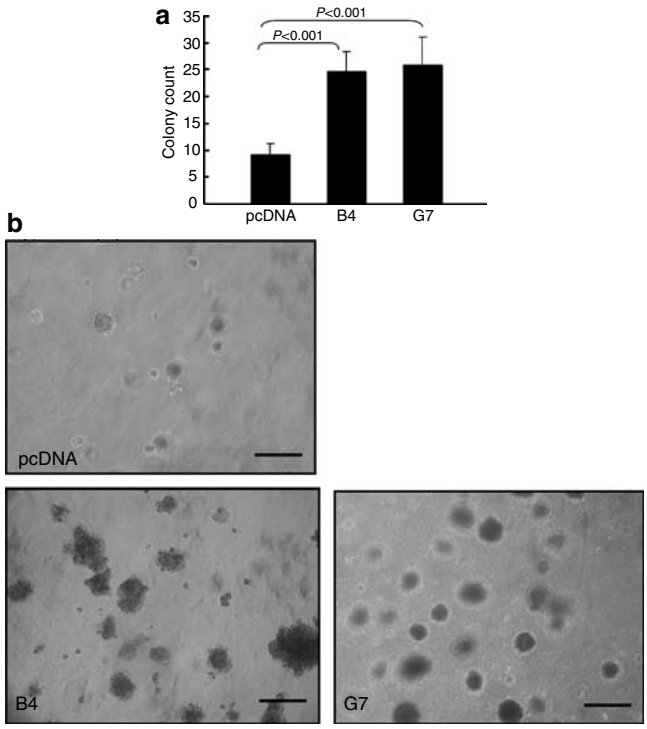

Figure 6. Anchorage-independent growth of COX-2-overexpressing BCC clones. (**a**) Anchorage-independent growth of COX-2-transfected BCC cells. A total of 1×10^3 cells were mixed in 0.35% soft agar and plated in a 3.5 cm diameter plate. Twenty eight days after seeding, the number of colonies was determined. Results shown are the mean ± SD of three experiments. (**b**) Colony morphology of COX-2 overexpression clones (B4 and G7) and vector control (pcDNA) cells. Bar = 0.2 mm.

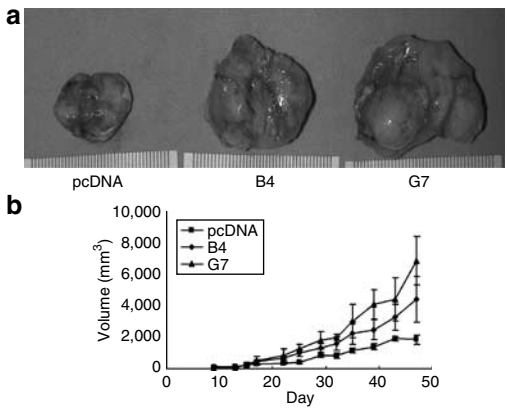

Figure 7. Tumorigenic effect of COX-2-overexpressing BCC cells in SCID mice. The vector control and COX-2-overexpressing clones (B4 and G7) were injected into SCID mice by subcutaneous inoculation of 5×10^6 cells (four mice per group). (**a**) The gross appearance of the xenograft following the killing of SCID mice performed 7 weeks after injection of BCC cells (**a**) and tumor size were assessed as described in Materials and Methods (**b**). Four independent experiments were performed. Significance was assessed using the Kruskal–Wallis equality of populations rank test.

between the level of expression of COX-2 and the density of tumor microvessels (8.96 ± 2.26 vessels/microscopic field for B4 cells, $n = 5$, $P < 0.05$, 8.22 ± 1.25 vessels/microscopic field for G7 cells, $P < 0.05$, $n = 5$ *vs* 4.46 ± 0.77

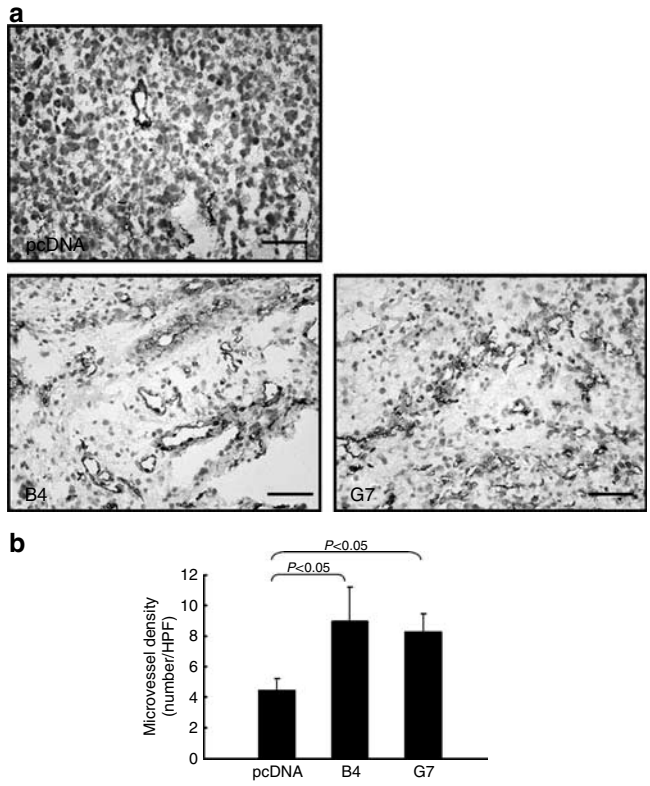

Figure 8. Microvessel density was increased in COX-2-overexpressing xenografts. (**a**) Immunohistochemical staining of sections of xenografts using anti-CD31 antibody. (**b**) Quantitative analysis of CD31-positive vessels (mean ± SD) by the standard method of microvessel density determination. pcDNA: vector control; B4 and G7: COX-2-overexpressing BCC clones. Bar = 50 μm.

vessels/microscopic field for pcDNA cells, $n = 5$) (Figure 8a and b).

DISCUSSION

Accumulated evidence suggests that cancer cells expressing higher levels of COX-2 may obtain a survival advantage that eventually facilitates tumor development and progression (Dannenberg *et al.*, 2005). We have shown that IL-6 overexpression in BCC cells increases expression of COX-2 and is accompanied by high vascularization (Jee *et al.*, 2001). Blockage of COX-2 function by siRNA abrogates IL-6-mediated angiogenic activities (Jee *et al.*, 2004) in a manner consistent with a downstream COX-2 effect of IL-6-induced angiogenesis in BCC cells. Several reports described that BCC had a low positive rate for COX-2 immunohistochemical staining in tested biopsies (Muller-Decker *et al.*, 1999; Kagoura *et al.*, 2001; Vogt *et al.*, 2001; Akita *et al.*, 2004). But recently, O'Grady *et al.* (2004) showed a positive staining of COX-2 in BCC, and demonstrated that COX-2 expression was correlated with microvessel densities. We found that higher levels of COX-2 expression not only associated with neovascularization but also correlated with tumor invasion depth in human BCC specimens (manuscript in submission).

In the present study, we demonstrate the function of COX-2 in tumorigenesis and angiogenesis by both molecular dissection and *in vivo* inspection. COX-2 is an enzyme that mediates many physiological functions, such as inhibition of cell apoptosis, augmentation of angiogenesis, and increased cell motility. The COX-2-mediated functions are influenced in part by various genes such as VEGF-A (Ma *et al.*, 2002), CD44, and matrix metalloproteinases (Dohadwala *et al.*, 2002). High COX-2 levels in the human colon (Tsujii *et al.*, 1998) and gastric cancers (Jones *et al.*, 1999) greatly promote tumor growth by increasing microvessel density (ie angiogenesis). VEGF-A is a major downstream effecter gene of COX-2-induced angiogenesis in colon cancer (Seno *et al.*, 2002). Recently, it was shown in Apc/COX-2 double knockout mice that stromal expression of COX-2 is required for the induction of VEGF and subsequent tumor angiogenesis (Seno *et al.*, 2002). Tumors in COX-2 knockout mice showed decreased expression of VEGF mRNA and a 30% decrease in vascular density compared with wild type (Williams *et al.*, 2000). Loss of wild-type p53, a tumor suppressor gene, is associated with increased expression of COX-2 mRNA and increased release of bFGF (Galy *et al.*, 2001) and VEGF (Yuan *et al.*, 2002). The product of COX-2 enzymatic function, PGE_2, stimulates VEGF production by promoting the translocation of hypoxia-inducible factor-α from cytosol to nucleus (Liu *et al.*, 2002). PGE_2 was reported to induce the accumulation of IL-8 mRNA and protein production in human colonic epithelial cells (Yu and Chadee, 1998). PGE_2 induces IL-8 mRNA transcription through PGE_2 receptor 1- and 4-dependent signal transduction pathway in human T cells (Caristi *et al.*, 2005). IL-8 is well known for its angiogenesis capability in many human cancers. Our study revealed that there are slight increases in IL-8 mRNA levels in COX-2-overexpressing clones (varying from 1.1- to 1.6-fold), whereas VEGF-A showed a more prominent increase in mRNA (1.8- to 2.4-fold). Secreted bFGF was also increased markedly in COX-2-overexpressing clones, by ELISA. Therefore, in addition to VEGF-A and bFGF, the role of IL-8 in mediating angiogenesis in COX-2-overexpressing BCC is worthy of further investigation.

Several apoptosis regulators were examined in our study. Mcl-1 and Bcl-2, both members of Bcl-2 family, were significantly upregulated in COX-2-overexpressing BCC cells, whereas other Bcl-2 members were not. This implicates Mcl-1 and Bcl-2 in COX-2-mediated antiapoptotic effects. Overexpression of COX-2 on rat intestinal epithelial cells results in inhibition of apoptosis and overexpression of Bcl-2 (Tsujii and DuBois, 1995). Exposure of a variety of cancer cells to a selective COX-2 inhibitor induces apoptosis (Arico *et al.*, 2002; Elder *et al.*, 2002). One potential mechanism for the proapoptotic activity of COX-2 inhibitors is the downregulation of Bcl-2 (Sheng *et al.*, 1998). Tumor tissue expressed reduced levels of proapoptotic proteins Bax and Bcl-XL, and increased levels of the antiapoptotic protein Bcl-2 in COX-2 transgenic mice model. Decreased apoptosis of mammary epithelial cells contributes to tumorigenesis in COX-2-overexpressing transgenic mice (Liu *et al.*, 2001).

The Mcl-1 gene was originally identified as an early gene that is induced during differentiation of ML-1 myeloid leukemia cells (Kozopas *et al.*, 1993). Overexpression of Mcl-1 delays apoptosis via a broad array of agents, such as c-Myc overexpression, growth factor withdrawal, and other cytotoxic agents (Ando *et al.*, 1998; Chao *et al.*, 1998; Wang *et al.*, 1999). The intracellular distribution of Mcl-1 protein overlaps with that of Bcl-2 protein, with prominent mitochondrial membrane localization (Yang *et al.*, 1995). Previously, we demonstrated that Mcl-1 upregulation is involved in IL-6-mediated antiapoptotic effects. Recently, Mcl-1 expression has been shown to be upregulated by COX-2/PGE_2 in lung adenocarcinoma cell line (Lin *et al.*, 2001). Increased levels of Mcl-1 induced by the overexpression of COX-2 were reported in cholangiocarcinoma and lymphomas (Nzeako *et al.*, 2002; Wun *et al.*, 2004).

COX-2 is present in normal skin, benign epidermal proliferation, and malignant skin neoplasm (Buckman *et al.*, 1998; Kagoura *et al.*, 2001). Sun exposure is the essential causal factor of BCC. Acute exposure of human keratinocytes to UVB irradiation results in increased production of PGE_2 and increased expression of COX-2 (Buckman *et al.*, 1998). COX-2 protein expression is upregulated in the human epidermis after exposure to UVB (Buckman *et al.*, 1998). Chronic inflammation upregulates mediators of inflammatory response, such as COX-2, leading to the production of inflammatory cytokines and prostaglandins, which may suppress cell-mediated immune response and promote angiogenesis (O'Byrne and Dalgleish, 2001). Topical application of celecoxib also inhibits chronic inflammation and UVB-induced papilloma/carcinoma in Skh/hr mice (Wilgus *et al.*, 2003). Recently, COX-2 was reported as a target of treatment in conjunction with photodynamic therapy in many skin cancers (Akita *et al.*, 2004). Combination of 5-fluorouracil and celecoxib also displayed synergistic regression of UVB-induced skin tumors (Wilgus *et al.*, 2004). Our data showed that tumor aggressiveness, defined as a higher microvessel density and deeper local invasion depth, was associated with levels of COX-2 expression (manuscript in preparation). COX-2 thus might serve as a chemopreventive and therapeutic target in human skin cancers.

Finally, the present study reveals that COX-2 induces antiapoptotic activity and angiogenesis in BCC by upregulation of Bcl-2 and Mcl-1, as well as secreted VEGF-A and bFGF. The exact molecular mechanism and downstream effectors that mediate angiogenesis and tumorigenesis in COX-2-overexpressing cell line remain to be elucidated by a further genome-wide analysis. Our findings suggest that blocking COX-2 function may increase susceptibility to apoptosis and inhibit angiogenesis in BCC, thus providing a feasible scheme for treatment and prevention of human BCC. Further clinical trials may be needed to test the effectiveness of COX-2-specific inhibitor combined with chemotherapeutic agents or photodynamic therapy in the treatment of human BCC. COX-2 inhibition might have beneficial effects, especially for BCC with a higher level of COX-2 expression or aggressive phenotypes. We hope to find more specific therapeutic targets that can be useful in treatment of human BCC in the near future.

MATERIALS AND METHODS

The medical ethical committee of the National Taiwan University College of Medicine approved all described studies. The study was conducted according to the Declaration of Helsinki Principles.

Cell origin, cell culture, and establishment of COX-2 transfectants

The human BCC cell line (parental BCC cells, originally designated BCC-KMC-1) originated from an undifferentiated BCC derived from a trauma scar. The 130–135th passages of this cell line were used in this study. The pCMV-COX-2, a constitutive expression vector, carries full-length human *COX-2* cDNA under the control of the cytomegalovirus promoter/enhancer sequence and with a neomycin selection marker. The BCC cells were transfected with pCMV-COX-2 or control pcDNA3 vector (GIBCO Invitrogen Co., Grand Island, NY), containing a cytomegalovirus promoter and a neomycin selection marker, using the TransFast^{TM} transfection reagent (Promega Co., Madison, WI). After 24 hours, cells were replanted in RPMI 1640 medium (GibcoBRL, Rockville, MD) with 10% fetal calf serum and 500 ng/ml G418 (Sigma Chemical Co., St Louis, MO). The G418-resistant clones were selected and expanded. For this study, we used high-expression transfectants (B4, C5, E4, and G7), the parental BCC cells and BCC cells transfected with control vector (pcDNA) served as controls. All of these cells were grown at 37°C and 5% CO_2 in RPMI 1640 medium supplemented with 10% (vol/vol) fetal bovine serum.

Antibodies and reagents

Anti-Mcl-1 (BD Pharmingen, San Diego, CA), anti-Bcl-2 (BD Pharmingen), anti-Bcl-XL (Santa Cruz Biotechnology, Santa Cruz, CA), anti-BAD (Santa Cruz Biotechnology), anti-VEGF-A (R&D Systems, Minneapolis, MN), anti-COX-2 (Cayman Chemical, Ann Arbor, MI), and anti-α-tubulin antibody (NeoMarkers, Freemont, CA) were used in immunoblotting analysis. Neutralizing antibody (goat polyclonal anti-bFGF antibody) was obtained from R&D Systems. The NS-398, a COX-2-specific inhibitor, was obtained from Cayman Chemical (Ann Arbor, MI).

Apoptosis ELISA assay

A sensitive ELISA that detects cytoplasmic histone-associated DNA fragments was performed, according to the manufacturer's protocol (Cell Death Detection ELISAPLUS; Roche Diagnostic GmbH, Mannheim, Germany). Briefly, human BCC cell lines were cultured in 6 cm Petri dishes (10^6 cells/dish) overnight, then treated with UVB 25 mJ/cm^2 and harvested at 6 and 12 hours. An amount of 1×10^4 cells was then centrifuged at $200 \times g$. The cells were lysed with lysis buffer for 30 minutes, followed by centrifugation at $200 \times g$ for 10 minutes at room temperature. The supernatant was collected and incubated with immunoreagent for 2 hours. After washing, a substrate solution was added into each well and kept in the dark until the color developed. The reaction was determined in a spectrophotometry at 405 nm, with 490 nm as the reference wavelength. The result was presented as enrichment factor (EF). The EF is defined as mU of sample/mU of the corresponding negative control (mU = absorbance (10^{-3})).

Flow cytometry analysis

The BCC/COX-2 cells and vector controls (1×10^6) were treated with UVB 25 mJ/cm^2. At an indicated time, cells were harvested and fixed in 75% methanol at −20°C for at least 30 minutes. After centrifugation ($100 \times g$) for 5 minutes at 4°C, the cell pellets were resuspended in 1 ml of phosphate-buffered saline (PBS) containing 2 μg/ml RNase A and incubated for 30 minutes. Finally, propidium iodide solution was added to a final concentration of 40 μg/ml. Fluorescence emitted from the PI-DNA complex was quantified after laser excitation of the fluorescent dye using FACS flow cytometry (Becton-Dickinson, Labware, Bedford, MA).

Preparation of CM

Parental BCC, pcDNA, B4, or G7 cells were plated in 1 ml of culture medium at 2×10^5 cells/well in 24-well 18 mm culture dishes. After serum starvation for 1 day, the culture supernatants were collected 24 hours later and centrifuged sequentially at $12{,}500 \times g$ with Microcon YM-3 centrifugal filter devices (Millipore Co., Bedford, MA) (with the cutoff of molecules smaller than 3,000 Da) for 30 minutes to obtain a 10-fold concentrate culture supernatant.

Matrigel blood plug *in vivo* assay

Matrigel blood plug assay was performed as described previously (Plunkett and Hailey, 1990; O'Reilly *et al.*, 1997). Briefly, C57BL6j mice (five per group) were each injected subcutaneously with 50 μl of CM from various cell lines mixed with 450 μl Matrigel (growth factor reduced) (Becton-Dickinson, Labware, Bedford, MA) and 40 U heparin/ml at 4°C. Mice were killed 6 days later; gels were recovered and processed for further studies. Neovessels was quantified by Drabkin method, measuring hemoglobin of the plug with the Drabkin reagent kit 525 (Sigma, St Louis, MI).

In vitro capillary tube formation on Matrigel

Human umbilical vein was collected with consent. The HUVEC capillary tube formation was evaluated as follows. Twenty-four-well 18 mm tissue culture dishes were coated with Matrigel basement membrane matrix (300 μl/well) (Becton-Dickinson) at 4°C and allowed to polymerize at 37°C for at least 30 minutes. The HUVECs (5×10^4 cells/well, in 24-well 18 mm tissue culture dishes) were grown in a final volume of 0.4 ml culture medium containing 150 μl M199 (GibcoBRL, Rockville, MD) and 250 μl CM. After 6 hours incubation, tube formation was observed through an inverted, phase-contrast photomicroscope, then photographed and counted. The number of tube formations was measured by counting the number of tube-like structures formed by connected endothelial cells in five randomly selected 9.7 mm^2 microscopic fields. The assay was performed in triplicate.

COX-2-specific RNA interference

The target sequence for the *COX-2* siRNA was bases 291–313 of NM000963.1 (5′-aactgctcaacaccggaattttt-3′) following the description by Denkert *et al.* (2003). The pRNA-U6/neo (GenScript Corp., Piscataway, NJ) is an siRNA expression vector with neomycin as the selection marker. We constructed pRNA-U6/COX-2, a constitutively expressed vector, which carries the *COX-2* siRNA sequence under the control of U6 promoter. The BCC/COX-2 cells were transiently transfected with pRNA-U6/COX-2 overnight. Inhibition of COX-2 protein was confirmed by Western blotting and function inhibition was measured by the PGE_2 EIA kit.

Reverse transcriptase-PCR

The RNAs from BCC/COX-2 and vector control were isolated using Trizol followed by chloroform. The mixture was then centrifuged, which yielded an upper aqueous phase containing total RNA. After precipitation with isopropanol, the RNA pellet was redissolved in denaturing solution, reprecipitated with isopropanol, and washed with 75% ethanol. An amount of 5 μg of total RNA was subjected to first-strand synthesis using Random Hexamer (Promega, Madison, WI) and M-MLV Reverse Transcriptase (RNase H Minus) (Promega, Madison, WI) at 37°C for 3 hours. The cDNA was then diluted to a final volume of 20 μl and quantified. Each 1 μl PCR reaction contained *Taq* polymerase (0.5 U/l; Protech Technology, Taipei, Taiwan) and 25 pmol each of the sense and the antisense primers in PCR buffer (10 mM Tris pH 9, 50 mM KCl, 6 mM $MgCl_2$, 0.01% gelatin, and 0.1% Triton X-100). Primer sequences are as follows: IL-8: sense 5′-CTC TCT TGG CAG CCT TCC TGA TT-3′ and antisense 5′-AAC TTC TCC ACA ACC CTC TGC AC-3′; VEGF-A: sense 5′-AGC TAC TGC CAT CCA ATC GC-3′ and antisense 5′-GGG CGA ATC CAA TTC CAA GAG-3′; platelet-derived growth factor: sense 5′-AAG CAT GTG CCG GAG AAG CG-3′ and antisense 5′-TCC TCT AAC CTC ACC TGG AC-3′; bFGF: sense 5′-AGT CTC CTG GAG AAA GCT-3′ and antisense 5′-CCC TTG ATG GAC ACA ACT-3′; and β-actin: sense 5′-CGT CTG GAC CTG GCT GGC CGG GAC C-3′ and antisense 5′-CTA GAA GCA TTT GCG GTG GAC GAT G-3′. The reaction mixture was incubated for 5 minutes at 94°C and then amplified by 25 PCR cycles (denaturing for 1 minute at 94°C, annealing for 1 minute at 56°C, and extending for 1 minute at 72°C). Each PCR product was then analyzed on a 2% agarose gel stained with 1 μg/ml ethidium bromide and photographed (Syngene; Syngene Bio Imaging System). Intensity of bands on the photographs was quantified by scanning laser densitometry.

Enzyme immunoassay (ELISA)

The PGE_2 EIA kit (Cayman Chemical, Ann Arbor, MI) and bFGF and VEGF ELISA kits (R&D Systems) were used to determine the respective levels of PGE_2, bFGF, and VEGF in cell culture supernatants. Each measurement was carried out according to the manufacturer's instructions, and each experiment was repeated in triplicate.

Western blot analysis

Cell lysates were prepared as described previously (Kuo *et al*., 1998). A 50 μg sample of each lysate was subjected to electrophoresis on a 10% SDS-polyacrylamide gel for detection of Mcl-1, Bcl-2, Bax, Bcl-x/L, VEGF-A, and COX-2. The samples were then electroblotted onto nitrocellulose paper. After blocking, blots were incubated with anti-Mcl-1, anti-Bcl-2, anti-Bax, anti-Bcl-x/L, anti-VEGF, and anti-Cox-2 antibodies in PBS containing Triton X-100 (PBST) for 1 hour followed by two washes (15 minutes each) in PBST. The samples were then incubated with horseradish peroxidase-conjugated goat anti-mouse IgG for 30 minutes. After washing, blots were incubated for 1 minute with the Western blotting reagent ECL (Amersham Biosciences UK Limited, Buckinghamshire, England) and chemiluminescence was detected by exposing the filters to Kodak-X-Omat films for 30 seconds to 3 minutes.

Colony growth in soft agar

Growth in soft agar was determined in six-well 35 mm diameter dishes prepared with a lower layer of 0.7% agar solution in RPMI with 10% fetal bovine serum, then overlaid with a 0.35% agar solution, also in growth medium, in which 1×10^6 cells were resuspended. Colonies were scored 28 days after preparation. (The colonies larger than 0.1 mm in diameter were scored as positive.) The pcDNA (vector control), B4, and G7 (COX-2-overexpressing clones) were subjected for colony formation assays.

Tumorigenicity assay in SCID mice. The SCID mice purchased from Tzu-Chi University Animal Center in Taiwan were housed in a dedicated SCID mouse facility with microisolator caging. The mice were handled under a unidirectional laminar airflow hood. Control-transfected BCC cells (pcDNA) and COX-2-transfected BCC cells (B4 and G7 clones) were trypsinized, washed with PBS, resuspended in PBS, and adjusted to a concentration of 5×10^6 cells/100 μl in PBS. The cell suspensions were then mixed with an equal volume of Matrigel before subcutaneous injection into SCID mice. Tumor development was followed in individual animals (four per group) by weekly sequential caliper measurements of length (L), width (W), and depth (H). Tumor volume was calculated by the formula $L \times W \times H \times 0.5236$. After 7 weeks, the mice were killed; the tumors were removed and weighed. A segment of the tumor was excised and fixed either in OCT embedding medium (Sakura Finetek USA Inc., Torrance, CA) or 10% neutral buffered formalin.

CONFLICT OF INTEREST

The authors state no conflict of interest.

ACKNOWLEDGMENTS

This work was supported by grants from National Science Council, Taiwan (NSC92-2314-B-002-156, NSC-93-2314-B-002-072, and NSC-93-3112-B-002-034) and a private donation from Mr Chao-Chai Lin.

REFERENCES

Akita Y, Kozaki K, Nakagawa A, Saito T, Ito S, Tamada Y *et al.* (2004) Cyclooxygenase-2 is a possible target of treatment approach in conjunction with photodynamic therapy for various disorders in skin and oral cavity. *Br J Dermatol* 151:472–80

Ando T, Shibata H, Suzuki T, Kurihara I, Hayashi K, Hayashi M *et al.* (1998) The possible role of apoptosis-suppressing genes, bcl-2 and mcl-1/EAT in human adrenal tumors. *Endocr Res* 24:955–60

Arico S, Pattingre S, Bauvy C, Gaine P, Barbat A, Codogno P *et al.* (2002) Celecoxib induces apoptosis by inhibiting 3-phosphoinositide-dependent protein kinase-1 acitivty in the human colon cancer HT-29 cell line. *J Biol Chem* 277:27613–21

Buckman SY, Gresham A, Hale P, Hruza G, Anast J, Masferrer J *et al.* (1998) COX-2 expression is induced by UVB exposure in human skin: implications for the development of skin cancer. *Carcinogenesis* 19:723–9

Caristi S, Piraino G, Cucinotta M, Valenti A, Loddo S, Teti D (2005) Prostaglandin E2 induces interleukin-8 gene transcription by activating C/EBP homologous protein in human T lymphocytes. *J Biol Chem* 280:14433–42

Chao JR, Wang JM, Lee SF, Peng HW, Lin YH, Chou CH *et al.* (1998) mcl-1 is an immediate-early gene activated by the granulocyte–macrophage colony-stimulating factor (GM-CSF) signaling pathway and is one component of the GM-CSF viability response. *Mol Cell Biol* 18:4883–98

Dannenberg AJ, Lippman SM, Mann JR, Subbaramaiah K, DuBois RN (2005) Cyclooxygenase-2 and epidermal growth factor receptor: pharmacologic targets for chemoprevention. *J Clin Oncol* 23:254–66

de Gruijl FR, van Kranen HJ, Mullenders LH (2001) UV-induced DNA damage, repair, mutations and oncogenic pathways in skin cancer. *J Photochem Photobiol* 63:19–27

Dempke W, Rie C, Grothey A, Schmoll HJ (2001) Cyclooxygenase-2: a novel target for cancer therapy? *J Cancer Res Clin Oncol* 27:411–7

Denkert C, Furstenberg A, Daniel PT, Koch I, Kobel M, Weichert W *et al.* (2003) Induction of G0/G1 cell cycle arrest in ovarian carcinoma cells by the anti-inflammatory drug NS-398, but not by COX-2-specific RNA interference. *Oncogene* 22:8653–61

Dohadwala M, Batra RK, Luo J, Lin Y, Krysan K, Pold M *et al.* (2002) Autocrine/paracrine prostaglandin E2 production by non-small cell lung cancer cells regulates matrix metalloproteinase-2 and CD44 in cyclooxygenase-2 dependent invasion. *J Biol Chem* 277:50828–33

Elder DJ, Halton DE, Playle LC, Paraskeva C (2002) The MEK/ERK pathway mediates COX-2-selective NSAID-induced apoptosis and induced COX-2 protein expression in colorectal carcinoma cells. *Int J Cancer* 99: 323–7

Fischer SM, Lo HH, Gordon GB, Seibert K, Kelloff G, Lubet RA *et al.* (1999) Chemopreventive activity of celecoxib, a specific cyclooxygenase-2 inhibitor and indomethacin against ultraviolet light-induced skin carcinogenesis. *Mol Carcinog* 25:231–40

Galy B, Creancier L, Zanibellato C, Prats AC, Prats H (2001) Tumour suppressor p53 inhibits human fibroblast growth factor 2 expression by a post-transcriptional mechanism. *Oncogene* 20:1669–77

Jee SH, Chu CY, Chiu HC, Huang YL, Tsai WL, Liao YH *et al.* (2004) Interleukin 6 induced basic fibroblast growth factor dependent angiogenesis in basal cell carcinoma cell line via JAK/STAT3 and PI3-kinase/Akt pathways. *J Invest Dermatol* 123:1169–75

Jee SH, Shen SC, Chiu HC, Tsai WL, Kuo ML (2001) Overexpression of interleukin-6 in human basal cell carcinoma cell lines increases anti-apoptotic activity and tumorigenic potency. *Oncogene* 20: 198–208

Jones MK, Wang H, Peskar BM, Levin E, Itani RM, Sarfeh IJ *et al.* (1999) Inhibition of angiogenesis by nonsteroidal anti-inflammatory drugs: insight into mechanisms and implications for cancer growth and ulcer healing. *Nat Med* 5:1418–23

Kagoura M, Toyoda M, Matsui C, Morohashi M (2001) Immunohistochemical expression of cyclooxygenase-2 in skin cancers. *J Cutan Pathol* 28:298–302

Kozopas KM, Yang T, Buchan HL, Zhou P, Craig RW (1993) MCL-1, a gene expressed in programmed myeloid cell differentiation, has sequence similarity to BCL2. *Proc Natl Acad Sci USA* 90:3516–20

Kuo ML, Shen SC, Yang CH, Chuang SE, Cheng AL, Huang TS (1998) Bcl-2 prevents topoisomerase II inhibitor GL331-induced apoptosis is mediated by down-regulation of poly(ADP-ribose)polymerase activity. *Oncogene* 17:2225–34

Lin MT, Lee RC, Yang PC, Ho FM, Kuo ML (2001) Cyclooxygenase-2 inducing Mcl-1-dependent survival mechanism in human lung adenocarcinoma CL1.0 cells. Involvement of phosphatidylinositol 3-kinase/Akt pathway. *J Biol Chem* 276:48997–9002

Liu CH, Chang SH, Narko K, Trifan OC, Wu MT, Smith E *et al.* (2001) Overexpression of cyclooxygenase-2 is sufficient to induce tumorigenesis in transgenic mice. *J Biol Chem* 276:18563–9

Liu XH, Kirschenbaum A, Lu M, Yao S, Dosoretz A, Holland JF *et al.* (2002) Prostaglandin E2 induces hypoxia-inducible factor-1 alpha stabilization and nuclear localization in a human prostate cancer cell line. *J Biol Chem* 277:50081–6

Ma L, del Soldato P, Wallace JL (2002) Divergent effects of new cyclooxygenase inhibitors on gastric ulcer healing: shifting the angiogenic balance. *Proc Natl Acad Sci USA* 99:13243–7

Miller DL, Weinstock MA (1994) Nonmelanoma skin cancer in the United States: incidence. *J Am Acad Dermatol* 30:774–8

Muller-Decker K, Neufang G, Berger I, Neumann M, Marks F, Furstenberger G (2002) Transgenic cyclooxygenase-2 overexpression sensitizes mouse skin for carcinogenesis. *Proc Natl Acad Sci USA* 99:12483–8

Muller-Decker K, Reinerth G, Krieg P, Zimmermann R, Heise H, Bayerl C *et al.* (1999) Prostaglandin-H-synthease isozyme expression in normal and neoplastic human skin. *Int J Cancer* 82:648–56

Muller-Decker K, Scholz K, Marks F, Furstenberger G (1995) Differential expression of prostaglandin H synthase isozymes during multistage carcinogenesis in mouse epidermis. *Mol Carcinog* 12:31–41

Nzeako UC, Guicciardi ME, Yoon JH, Bronk SF, Gores GJ (2002) COX-2 inhibits Fas-mediated apoptosis in cholangiocarcinoma cells. *Hepatology* 35:552–9

O'Byrne KJ, Dalgleish AG (2001) Chronic immune activation and inflammation as the cause of malignancy. *Br J Cancer* 85:473–83

O'Grady A, O'Kelly P, Murphy GM, Leader M, Kay E (2004) COX-2 expression correlates with microvessel density in non-melanoma skin cancer from renal transplant recipients and immunocompetent individuals. *Hum Pathol* 35:1549–55

O'Reilly MS, Boehm T, Shing Y, Fukai N, Vasios G, Lane WS *et al.* (1997) Endostatin: an endogenous inhibitor of angiogenesisand tumor growth. *Cell* 88:277–85

Plunkett ML, Hailey JA (1990) An *in vivo* quantitative angiogenesismodel using tumor cells entrapped in alginate. *Lab Invest* 62:510–7

Seno H, Oshima M, Ishikawa TO, Oshima H, Takaku K, Chiba T *et al.* (2002) Cyclooxygenase 2- and prostaglandin E(3) receptor EP(2)-dependent angiogenesis in Apc(Delta716) mouse intestinal polyps. *Cancer Res* 62:506–11

Seo JY, Kim EK, Lee SH, Park KC, Kim KH, Eun HC *et al.* (2003) Enhanced expression of cylooxygenase-2 by UV in aged human skin *in vivo*. *Mech Ageing Dev* 124:903–10

Sheng H, Shao J, Morrow JD, Beauchamp RN, DuBois RN (1998) Modulation of apoptosis and Bcl-2 expression by prostaglandin E2 in human colon cancer cells. *Cancer Res* 58:362–6

Taketo MM (1998) Cyclooxygenase-2 inhibitors in tumorigenesis (part II). *J Natl Cancer Inst* 90:1609–20

Tsujii M, DuBois RN (1995) Alterations in cellular adhesion and apoptosis in epithelial cells overexpressing prostaglandin endoperoxide synthase 2. *Cell* 83:493–501

Tsujii M, Kawano S, Tsuji S, Sawaoka H, Hori M, DuBois RN (1998) Cyclooxygenase regulates angiogenesis induced by colon cancer cells. *Cell* 93:705–16

Vogt T, McClelland M, Jung B, Popova S, Bogenrieder T, Becker B *et al.* (2001) Progression and NSAID-induced apoptosis in malignant melanomas are independent of cyclooxygenase II. *Melanoma Res* 11:587–99

Wang JM, Chao JR, Chen W, Kuo ML, Yen JJ, Yang-Yen HF (1999) The antiapoptotic gene mcl-1 is up-regulated by the phosphatidylinositol 3-kinase/Akt signaling pathyway through a transcription factor complex containing CREB. *Mol Cell Biol* 19:6195–206

Wilgus TA, Breza TS Jr, Tober KL, Oberyszyn TM (2004) Treatment with 5-fluorouracil and celecoxib displays synergistic regression of ultraviolet light B-induced skin tumors. *J Invest Dermatol* 122:1488–94

Wilgus TA, Koki AT, Zweifel BS, Kusewitt DF, Rubal PA, Oberyszyn TM (2003) Inhibition of cutaneous ultrabiolet light B-mediated inflammation and tumor formation with topical celecoxib treatment. *Mol Carcinog* 38:49–58

Williams CS, Tsujii M, Reese J, Dey SK, DuBois RN (2000) Host cyclooxygenase-2 modulate carcinoma growth. *J Clin Invest* 105:1589–94

Wun T, McKnignt H, Tuscano JM (2004) Increased cyclooxygenase-2 (COX-2): a potential role in the pathogenesis of lymphoma. *Leuk Res* 28:179–90

Yang T, Kozopas KM, Craig RW (1995) The intracellular distribution and pattern of expression of Mcl-1 overlap with but are not identical to, those of Bcl-2. *J Cell Biol* 128:1173–84

Yu Y, Chadee K (1998) Prostaglandin E2 stimulates IL-8 gene expression in human colonic epithelial cells by a posttranscriptional mechanism. *J Immunol* 161:3746–52

Yuan A, Yu CJ, Luh KT, Kuo SH, Lee YC, Yang PC (2002) Aberrant p53 expression correlates with expression of vascular endothelial growth factor mRNA and interleukin-8 mRNA and neoangiogenesis in non-small cell lung cancer. *J Clin Oncol* 20:900–10